

# Melt-Enhanced Rejuvenation of Lithospheric Mantle: Insights from the Colorado Plateau

Mousumi Roy<sup>a</sup>, Rodrigo Osuna Orozco<sup>a,c</sup>, Ben Holtzman<sup>b</sup>, James Gaherty<sup>b</sup>

<sup>a</sup>*Department of Physics and Astronomy, University of New Mexico, Albuquerque, NM 87106, USA.*

<sup>b</sup>*Lamont Doherty Earth Observatory, Columbia University, Palisades, NY 10964, USA.*

<sup>c</sup>*now at Scripps Institution of Oceanography, University of California San Diego, La Jolla, CA 92037, USA.*

---

## Abstract

The stability of the lithospheric mantle beneath the ancient cratonic cores of continents is primarily a function of chemical modification during the process of melt extraction. Processes by which stable continental lithosphere may be destabilized are not well-understood, although destabilization by thickening and removal of negatively-buoyant lithospheric mantle in “delamination” events has been proposed in a number of tectonic settings. In this paper we explore an alternative process for destabilizing continents, namely, thermal and chemical modification during infiltration of metasomatic fluids and melts into the lithospheric column. We consider observations pertinent to the structure and evolution of the Colorado Plateau within the western United States to argue that the physical and chemical state of the margins of the plateau have been variably modified and destabilized by interaction with melts. In the melt-infiltration process explored here, the primary mechanism for weakening and rejuvenating the plate is through thermal effects and the feedback between deformation and melt-infiltration. We speculate on the nature and geometry of a melt-modulated interaction zone between lithosphere

and asthenosphere and the seismically-observable consequences of variable melt-infiltration into the margins of regions of thick, stable lithosphere such as the Colorado Plateau and the Archean Wyoming Province within North America.

*Keywords:* melt-infiltration, cratons, Colorado Plateau, rejuvenation

---

## 1. Introduction

It has long been recognized that the sub-continental lithospheric mantle plays an important role in stabilizing tectonic plates against disruption. The stability of the lithospheric mantle beneath continents is primarily a function of its thermal structure and buoyancy modification by melt extraction (Lee et al., 2001; Lenardic et al., 2003). It is also widely recognized that stable continental lithosphere may be destabilized by a disruption of its buoyancy and thermal structure, for example, associated with thickening and removal of dense lithospheric mantle in “delamination” events (Elkins-Tanton, 2005; Molnar and Jones, 2004) as suggested in the Sierra Nevada (Zandt and Carrigan, 1993) and elsewhere in the western US (West et al., 2009; Schmandt and Humphreys, 2010; Levander et al., 2011). We explore an alternative process by which stable tectonic regions may be destabilized, namely, thermal and chemical modification during infiltration of melts into the lithospheric column. The potential importance of this “rejuvenation” process has been described in several peridotite massifs (Bodinier et al., 2008; Leroux et al., 2008; Soustelle et al., 2009; Marchesi et al., 2010) as the migration of a “refertilization” front that is driven by chemical and physical disequilibrium between infiltrating fluids and the surrounding lithosphere. In this work, we

20 use the terms refertilization and rejuvenation, with emphasis on the chemical  
21 and mechanical implications, respectively, and will explore the regional-scale  
22 geodynamic factors that control the process. Unless otherwise specified, we  
23 use the term lithosphere to signify the thermal boundary layer, although  
24 we will occasionally specify the compositionally-distinct chemical boundary  
25 layer when discussing xenolith data (Fischer et al., 2010).

26 This work is motivated by observations pertinent to the structure and  
27 Cenozoic evolution of the Colorado Plateau that suggest rejuvenation by  
28 interaction with melts. First, the Colorado Plateau has been minimally af-  
29 fected by deformation and magmatism during Cenozoic time, but there is ev-  
30 idence for active deformation at its margins (Figure 1; Berglund et al. (2012);  
31 Kreemer et al. (2010)). The internal strength of the Colorado Plateau has  
32 been attributed to a greater degree of iron-depletion, evidenced by mantle  
33 xenoliths with iron-magnesium ratios that are similar to those in Archean  
34 cratons and are distinct from those in surrounding regions (Alibert, 1990;  
35 Smith, 2000; Lee et al., 2001; Roy et al., 2009). The margins of the plateau  
36 however show evidence for Cenozoic deformation and have been affected by  
37 a slow encroachment of magmatic activity toward the plateau-interior since  
38 40 Ma (Roy et al., 2009; Wenrich et al., 1995). Seismic observations reveal  
39 slower wave speeds in the mantle at the margins of the plateau (Schmandt  
40 and Humphreys, 2010; Humphreys and Dueker, 1994; Goes and van der Lee,  
41 2002; Gao et al., 2004; Sine et al., 2008; Li et al., 2007; Tian et al., 2009) and  
42 higher  $V_p/V_s$  ratios at the margins relative to the plateau interior (Schmandt  
43 and Humphreys, 2010). Average surface heat flow for the margins of the  
44 plateau are comparable to values in the Basin and Range province (85-102

45 mW/m<sup>2</sup>), whereas average surface heat flow in the interior is lower (55-69  
46 mW/m<sup>2</sup>; Eggleston and Reiter, 1984; Swanberg and Morgan, 1985).

47 Higher seismic wavespeeds and lower heat flow in the interior of the Col-  
48 orado Plateau, together with the composition and thermobarometry of xeno-  
49 liths entrained in Cenozoic volcanics, indicate thick thermal and chemical  
50 lithosphere (Smith, 2000; Lee et al., 2001; Roy et al., 2009). Lower seismic  
51 wavespeeds, higher heat flow, and greater magmatism and seismicity at the  
52 margins of the plateau relative to the interior suggest that the lithosphere  
53 beneath the margins of the plateau is distinct from that of the interior.  
54 Sharp lateral gradients in seismic wavespeeds between the NW plateau mar-  
55 gin (Utah Transition Zone) and the interior of the plateau (Schmandt and  
56 Humphreys, 2010; Gao et al., 2004; Sine et al., 2008; Li et al., 2007) have  
57 prompted the suggestion that the margins of the plateau have been me-  
58 chanically thinned or removed (e.g., Schmandt and Humphreys, 2010; van  
59 Wijk et al., 2010; Levander et al., 2011). We argue that these observations,  
60 together with rock uplift and stratigraphic data, are also consistent with  
61 thermal and chemical modification by melt-infiltration at the margins of the  
62 plateau (Figure 1). Mechanical erosion or thinning and removal could be  
63 part of this modification, but we focus on the thermo-chemical aspects of  
64 melt-infiltration as an end-member on a spectrum of processes.

65 Specifically, we propose a process that is controlled by interactions at the  
66 lithosphere-asthenosphere boundary as North America moves with respect to  
67 the underlying asthenosphere. The removal of the subducted Farallon plate  
68 from beneath North America in middle-Tertiary time provides an important  
69 physical perturbation to the lithosphere-asthenosphere system (Humphreys

70 et al., 2003), that essentially triggers the melt-infiltration process explored  
71 here. We present two lines of evidence for melt-infiltration as a driving mech-  
72 anism for lithospheric rejuvenation and destabilization at the margins of re-  
73 gions of thick lithosphere. First, a simple numerical formulation of two-phase  
74 flow shows that melts and metasomatic fluids would preferentially infiltrate  
75 and thus modify regions with a gradient in plate thickness, for example at the  
76 margins of regions of thick lithosphere. We predict that infiltration of melt  
77 into the margins of regions of thick lithosphere is asymmetric, with enhanced  
78 infiltration at the “upwind” margins of the protrusion, with limited to no in-  
79 filtration at the “downwind” side. This explains first-order patterns in the  
80 rates and asymmetry of magmatic encroachment at the Colorado Plateau.  
81 Second, based on experimental observations described below, we infer that  
82 the regions of greatest melt infiltration are likely to be regions of enhanced  
83 viscosity reduction and strain concentration. In the models presented here,  
84 we do not explicitly include coupling of deformation and fluid segregation and  
85 organization, but instead present heuristic arguments for the importance of  
86 this stress-driven feedback based on numerical and laboratory experiments.  
87 Finally, we speculate about the general importance of the melt-infiltration  
88 process explored here and its role in the regional evolution of the western  
89 US.

## 90 **2. Stress-driven melt-segregation and melt-infiltration**

91 The dynamic organization of melt during deformation is an area of active  
92 field, laboratory and theoretical research. In this work we make a distinction  
93 between stress-driven melt-segregation (SDS), which is the re-distribution

94 of melt at the grain-scale during deformation of a molten aggregate, and  
 95 the large-scale motion of melt relative to the surrounding rock, which we  
 96 refer to as melt infiltration and extraction. The characteristic length scale  
 97 for distinguishing these processes of melt-rock interaction is the compaction  
 98 length,  $\delta_c$ , which depends on the solid and fluid viscosities and the perme-  
 99 ability,  $\delta_c = \sqrt{\kappa(\zeta + 4/3\eta)/\mu}$ . For typical viscosity contrasts between melt  
 100 and the solid (e.g., melt shear viscosity  $\mu = 1$  Pa s, and surrounding rock  
 101 bulk and shear viscosity of  $\zeta$  and  $\eta = 10^{21}$  to  $10^{24}$  Pa s; see parameters in  
 102 Table 1), and reasonable rock permeabilities ( $\kappa = 10^{-15}$  to  $10^{-12}$  m<sup>2</sup>), the  
 103 compaction length scale for the upper mantle is on the order of  $\delta_c = 10^1$  to  
 104  $10^4$  m (McKenzie, 1984). In the following we divide our discussion into melt-  
 105 infiltration and extraction over regional tectonic scales (much larger than the  
 106 compaction length) and stress-driven melt segregation processes that are rel-  
 107 evant at the grain-scale up to the compaction length. Although this division  
 108 in terms of the compaction length scale is a convenient way to categorize  
 109 the physics of magma migration, we note that interaction between processes  
 110 across these two length scales will play an important role in melt migration  
 111 through the asthenosphere and deeper portions of the lithosphere.

112 *2.1. Idealized model of spatially-variable melt-infiltration and extraction*

113 On length scales that are large compared to the compaction length, we ex-  
 114 pect pressure-gradients within the deforming lithosphere-asthenosphere sys-  
 115 tem to drive melt-infiltration into the lithosphere and thus control the dis-  
 116 tribution of magmatic activity at the surface. To first order, the interac-  
 117 tions between melt and a deformable solid matrix may be treated as a cou-  
 118 pled problem involving flow of two interpenetrating fluids (McKenzie, 1984;

119 Spiegelman, 1993, 2003) consisting of a low-viscosity phase such as melt and a  
 120 high viscosity phase representing the matrix. Analytic solutions for the two-  
 121 phase flow problem exist in idealized cases (McKenzie, 1984; Spiegelman,  
 122 1993) and if porosity gradients are nearly zero, relative motion between the  
 123 solid and melt, or the melt extraction rate, is primarily driven by pressure  
 124 gradients

$$125 \quad -\frac{\mu\phi}{\kappa_\phi}(\mathbf{v} - \mathbf{u}) = \nabla P - \rho_f \mathbf{g} \quad (1)$$

126 where we explicitly note that permeability may be a function of porosity,  
 127  $\mathbf{u}$  is the melt velocity, and  $\mathbf{v}$  is solid velocity (McKenzie, 1984; Spiegelman,  
 128 1993). Although these assumptions are simplistic, they define a first-order  
 129 approach to understanding how buoyancy-driven flow of melt will interact  
 130 with dynamic pressure gradients within the asthenosphere and lithosphere  
 131 to drive spatially-variable melt extraction rates.

### 132 *2.1.1. Melt organization due to variable lithosphere thickness*

133 We first consider a scenario in which a region of variable-thickness litho-  
 134 sphere (represented by a high-viscosity Newtonian fluid,  $\eta = \eta_l$ ) protrudes  
 135 into and moves relative to an asthenospheric “wind” (of a lower viscosity  
 136 Newtonian fluid,  $\eta = \eta_a$ ). The Couette-style shear between the plate and  
 137 the underlying mantle is modified by flow around the lithospheric protru-  
 138 sion(s) (Figure 2a and b). This flow field may represent, for example, either  
 139 eastward-driven asthenosphere or westward migration of the North Amer-  
 140 ican plate relative to the asthenospheric mantle. The keel-like protrusion  
 141 represents a region of thicker than average lithosphere, such as the Colorado  
 142 Plateau. If the viscosity contrast between the lithosphere and asthenosphere

143 is large (in these calculations  $\eta_l/\eta_a = 10^{3-4}$ ; Figure 2c), the keel-like protrusion  
144 will not deform greatly and the asthenospheric flow produces a “pressure  
145 shadow” effect within the keel: lower dynamic pressure on the upwind side  
146 of the keel and higher on the downwind side (Figure 3a). A similar effect is  
147 produced for 2D models of semicircular and periodic sinusoidal ridges at the  
148 base of the plate (Figure 3b).

149 For simplicity, we ignore processes that generate partial-melt in the lithosphere-  
150 asthenosphere system, but assume instead that a small, uniform melt-fraction  
151 is present everywhere within the model domain. In this case, equation (1)  
152 may be used to determine the melt extraction field: relative motion between  
153 the melt and the solid is driven by the competition between dynamic pressure  
154 gradients and buoyancy (right-hand side of equation 1). In the absence of  
155 dynamic pressure gradients (no deformation in the lithosphere and asthenosphere),  
156 the buoyancy term will drive upward motion of melt relative to the  
157 solid. If horizontal dynamic pressure gradients are sufficiently large, then  
158 melt motion relative to the solid will be more complicated. The geometry of  
159 the melt-extraction rate field is illustrated by calculating forward-streamlines  
160 for tracers that originate at a fixed depth, taken to be below the lithosphere  
161 protrusion(s) in our calculations (Figure 3). The effects of dynamic pressure  
162 gradients may be seen as the departure of the streamlines from vertical  
163 (buoyancy-dominated) orientation (Figure 3).

164 Asymmetry in the dynamic pressure gradients drive an asymmetry in  
165 melt-extraction on the upwind and downwind sides of the 3D hemispherical  
166 keel (Figure 3a) and also in the 2D models of semicircular and periodic ridges  
167 (Figure 3b). On the upwind side, asthenospheric flow diverges around the



168 protrusions and the upwind sector of the keel or ridge has lower dynamic  
169 pressure than the downwind sector (Figures 2 & 3). The dynamic pressure  
170 field thus focusses melt streamlines into the upwind sector of the protrusions  
171 and pushes them away from the downwind sector of the protrusions, produc-  
172 ing a pronounced upwind-downwind asymmetry due to asthenospheric flow  
173 (Figure 3).

#### 174 *2.1.2. Thermal effects of asthenosphere flow and melt-infiltration*

175 The models above solve the coupled Navier-Stokes and heat equations for  
176 a lithospheric region of high viscosity (hemisphere or ridges) that initially  
177 has a cool linear geotherm and an asthenospheric fluid with fixed, higher  
178 uniform temperature (1200 °C). The flow is accompanied by warming of the  
179 lithosphere, due to conduction (Roy et al., 2009) and advective heating by  
180 asthenospheric flow. We assume that the viscosities of the lithosphere and as-  
181 thenosphere are temperature-dependent (assuming  $\eta_l = \eta_0 \exp(-E(T - T_0))$ ),  
182 e.g., Zhong et al. (2000); parameters in Table 1) so that as the lithosphere  
183 warms, it weakens and deforms more easily. The deformation and dynamic  
184 pressure fields will evolve due to heating (Figure 4) and drive changes in  
185 the pattern of melt-extraction (Figure 4). At early times during the simu-  
186 lations the pattern of melt-extraction is asymmetric, with melt drawn into  
187 the upwind side and pushed out of the downwind side of the protrusions. In-  
188 terestingly, the surface pattern of asymmetric melt-extraction persists at the  
189 surface over timescales of  $10^7$  years for lithospheric protrusions with linear  
190 dimensions of  $10^2$  km across. At depth, however, warming and viscosity-  
191 reduction in the lithosphere causes diminishing gradients in dynamic pres-  
192 sure, so that melt-streamlines become increasingly vertical through time (Fig-

193 ure 4).

194 On the upwind side of the protrusion advective heating by the melt-  
195 infiltration enhances weakening of the lithosphere. At steady-state, assum-  
196 ing a constant melt-extraction field, advective heat transport by melt raises  
197 temperatures above background by around  $50 - 100^\circ\text{C}$  (see also Schmel-  
198 ing and Wallner, 2012). The additional heating would provide an important  
199 feedback between melt-infiltration and deformation, with melt-infiltration  
200 reducing plate viscosity by and additional  $\sim 40\%$ . The asymmetry in melt-  
201 extraction will drive an asymmetry in destabilization, namely the upwind  
202 side of the protruding lithosphere experiences this enhanced viscosity re-  
203 duction relative to the melt-free downwind sector. We predict, therefore,  
204 that lithospheric rejuvenation driven by melt-infiltration will be enhanced  
205 on the upwind sides of lithospheric protrusions. It is important to note that  
206 a more complete treatment of the problem will require not only this thermal  
207 feedback between melt-infiltration and plate viscosity, but also important  
208 feedbacks between melt-segregation and deformation observed in laboratory  
209 experiments at (and below) compaction length scales.

## 210 *2.2. Laboratory observations of melt and rheology at the meso-scale*

211 In deformation experiments on partially molten rocks, samples with ini-  
212 tially homogeneous melt distributions undergo a deformation-driven transi-  
213 tion where melt organizes into networks of connected, anastomosing shear  
214 zones (e.g., Kohlstedt and Holtzman, 2009). This process, referred to as  
215 stress-driven segregation (SDS), may provide an important feedback between  
216 melt distribution, transport, and rheology that controls the geometry and dis-  
217 tribution of melt. Laboratory experiments suggest that SDS is more likely

218 in higher-strain regions of the mantle, but the degree of strain and the feed-  
219 backs in an open system (and thus the volume in which the process occurs  
220 in the mantle) are not yet known. The notion of the compaction length,  
221 the characteristic length scale of coupling between solid matrix deformation  
222 and fluid flow, has been useful in predicting behavior in experiments (e.g.,  
223 Holtzman et al., 2003), and is consistent with the length scale of observed  
224 organized-melt structures when extrapolated from laboratory conditions to  
225 mantle and lower crust (e.g., Holtzman and Kohlstedt, 2007). For a region  
226 with homogeneous melt distribution the compaction length is uniform, but  
227 as melt organizes and segregates, at length scales smaller than that initial  
228 compaction length,  $\delta_c$  becomes spatially heterogeneous. Because the melt  
229 organization will produce anisotropic permeability and viscosity structures,  
230 the effective compaction length would also be anisotropic. While the char-  
231 acteristic spacing of the largest melt-rich features is predicted to be smaller  
232 than the compaction length, the linear dimensions of the volume in which  
233 the process occurs could be much larger than the initial compaction length.

234 In experiments starting from a homogeneous melt distribution, a degree  
235 of strain is required to segregate the melt to a point at which it begins to  
236 affect the rheological and melt-transport properties. This critical degree of  
237 strain,  $\gamma_c$ , shows some sensitivity to stress, and is thus likely to be a function  
238 of thermodynamic conditions. While previous work focused on the large  
239 bands that emerge by about a shear strain of  $\gamma = \pm 1$  as an indicator of  $\gamma_c$   
240 (Holtzman and Kohlstedt, 2007; Katz et al., 2006), Holtzman et al. (2012)  
241 demonstrate that the smallest scale bands form at much lower strains but  
242 cause a clear and immediate reduction of the effective viscosity. In Holtzman

243 and Kohlstedt (2007) it was proposed that the weakening is associated with  
244 high mobility of melt through a network of connected bands. The melt must  
245 form connected pathways, even if transiently, in order to reorganize easily  
246 to concentrate strain on low angle bands. Thus, the effective permeability is  
247 inferred to increase at the onset of weakening.

248 When extrapolating to an open system with thermal and compositional  
249 gradients, rapid melt transport can produce chemical and thermal disequi-  
250 librium between melt and host rock (Kohlstedt and Holtzman, 2009). The  
251 effects of chemical disequilibrium under gravity-driven melt flow has been well  
252 studied, especially in near-adiabatic conditions (e.g., Daines and Kohlstedt,  
253 1994; Kelemen et al., 1995). A method for exploring the coupling of SDS  
254 and chemical disequilibrium has demonstrated a strong coupling between  
255 the two, resulting in greatly enhanced infiltration (King et al., 2011b). Cal-  
256 culations in Holtzman et al. (2012), based on a model for permeability and  
257 its variation with degree of strain, suggest that SDS will enhance both the  
258 thermal and chemical disequilibrium in the rock volume. The potential feed-  
259 backs between thermal and chemical interactions and the microstructure of  
260 the rock (and thus the permeability) are not included in our model. While  
261 these disequilibrium processes are complex and difficult to predict, especially  
262 for open systems, we surmise that permeability would generally be enhanced  
263 in regions of SDS in the mantle.

264 To determine if and where the SDS process may occur in the mantle  
265 requires two approaches. The first is detailed scaling of the physics from  
266 laboratory- to mantle conditions (e.g., Takei and Hier-Majumder, 2009; King  
267 et al., 2011a; Butler, 2012). The second approach is to develop predic-

268 tive tests of dynamical consequences and observational signatures, such as  
269 the seismic velocity structure (e.g., Holtzman and Kendall, 2010; Takei and  
270 Holtzman, 2009) or electrical conductivity structure (Wannamaker et al.,  
271 2008). In our discussion below, we follow the second approach by combining  
272 insights from numerical models of melt extraction and experimental obser-  
273 vations to hypothesize on the role of melt-infiltration and its consequences  
274 for the Colorado Plateau and the western US.

### 275 **3. Discussion**

276 The models above, together with experimental observations of the be-  
277 havior of molten aggregates, suggest that melt-infiltration and stress-driven  
278 melt segregation must play an important role in the interaction of partial  
279 melts with the base of the lithosphere. To first-order, the geometry of  
280 the lithosphere-asthenosphere boundary controls dynamic pressure gradients  
281 due to deformation, which in turn control the spatial distribution of melt-  
282 extraction and observed magmatism. Regions with lateral variations in litho-  
283 sphere thickness will be characterized by complexity in the relative motion  
284 between the asthenosphere and lithosphere, as explored here for keel- and  
285 ridge-like lithospheric protrusions. Melt-infiltration preferentially occurs on  
286 the upwind side of regions of thick lithosphere, resulting in enhanced weaken-  
287 ing here and asymmetric thermal and chemical modification/rejuvenation of  
288 the lithosphere. Simultaneously high strain rates and melt-extraction rates in  
289 deforming parts of the protrusion will likely undergo SDS and form melt-rich,  
290 anastomosing shear zones, as observed in experiments. Although neither the  
291 model calculations nor the experimental observations discussed above address

292 the generation of partial-melt in the upper mantle, the Cenozoic evolution of  
293 the western US is characterized by a number of processes that can generate  
294 partial melting in the upper mantle beneath North America. We speculate,  
295 therefore, that SDS and melt-infiltration at the base of the lithosphere may  
296 profoundly control the distribution of magmatism and intra-plate deforma-  
297 tion in the western US.

### 298 *3.1. Application to the Colorado Plateau*

299 On a regional scale the spatial pattern of Cenozoic magmatism in the  
300 western US exhibits a magmatic gap across the Colorado Plateau, with the  
301 encroachment of the onset of magmatism inward toward the interior of the  
302 plateau on its NW, SW, and SE margins, with a distinct lack of encroach-  
303 ment on the NE margin (Roy et al., 2009). We argue that this pattern  
304 of magmatism may have occurred through a range of processes, both ther-  
305 mal and chemical, associated with melt-rock interaction at the lithosphere-  
306 asthenosphere boundary. Our models suggest that, among other factors,  
307 a protruding region of thicker lithosphere and accompanying regional scale  
308 dynamic pressure gradients may be responsible for organizing the surface  
309 distribution of magmatism surrounding and within the Colorado Plateau.  
310 In the context of specific observations at the Colorado Plateau, the melt-  
311 infiltration mechanism discussed here provides a unifying framework within  
312 which a number of disparate observations may be explained.

#### 313 *3.1.1. Spatio-temporal patterns of magmatism.*

314 We assume that the middle-Tertiary removal of the Farallon plate sub-  
315 jected the North America to a basal thermal perturbation (Roy et al., 2009;

316 Humphreys et al., 2003) and that relative motion between North America  
317 and the underlying asthenosphere has been steady since this time (Silver and  
318 Holt, 2002). In our models, the relative motion of North America over the  
319 underlying asthenosphere is the model is  $\sim 5$  cm/yr, comparable to rates  
320 inferred from the correlation between GPS-derived surface motions and seis-  
321 mic anisotropy (Silver and Holt, 2002). Additionally, upwelling flow in the  
322 asthenosphere in response to the sinking Farallon plate would drive both  
323 long-wavelength dynamic rock uplift (Moucha et al., 2008; Liu and Gurnis,  
324 2010) and generate accompanying partial melt in the asthenosphere beneath  
325 the western US. The voluminous and regionally-extensive middle-Tertiary  
326 ignimbrite flareup, for example, has been attributed to the removal of the  
327 Farallon slab and subsequent interaction between asthenospheric and litho-  
328 spheric partial melts (Humphreys et al., 2003). Thermal expansion due to  
329 conductive relaxation of isotherms following the removal of the Farallon slab  
330 is sufficient to explain a large fraction of the rock uplift of the Colorado  
331 Plateau and the rate of migration of the isotherms is comparable to (though  
332 slightly slower than) the observed slow rates of magmatic encroachment (3-6  
333 km/my) onto the plateau (Roy et al., 2009).

334 The models presented here refine the findings in Roy et al. (2009), where  
335 the Colorado Plateau is represented by a region where a deep keel of litho-  
336 sphere protrudes into the asthenosphere, around which the asthenosphere  
337 must flow. Our models offer an explanation for the observed asymmetry in  
338 magmatic encroachment surrounding the Colorado Plateau, which was not  
339 previously explained in the simpler conductive models of Roy et al. (2009).  
340 Specifically, we note that in a frame of reference stationary with respect to

341 North America, the asthenosphere below the plate is inferred to move in a  
342 roughly SW-NE direction (Figure 1). Consistent with our models, the highest  
343 rates of magmatic encroachment onto the plateau ( $\sim 6$  km/my) are observed  
344 in the upwind sector of the plateau (its SW quadrant), whereas magmatic  
345 encroachment occurs at a slower rate on the NW and SE quadrants (Roy  
346 et al., 2009). In contrast, the downwind sector (its NE quadrant, adjacent to  
347 the San Juan volcanic field and northern Rio Grande rift) shows a distinct  
348 lack of magmatic encroachment (Roy et al., 2009).

349 In our models, the expected rate at which the zone of melt focusing  
350 migrates into the upwind side of the protruding lithosphere is a function of  
351 time, ranging from values as high as 6 km/my to slower rates  $\sim 2 - 3$  km/my  
352 (Figure 5). These rates of migration of the magmatic zone are comparable  
353 to observed magmatic encroachment rates estimated by Roy et al. (2009)  
354 at the SW (6.3 km/my), NW (4.0 km/my) and SE (3.3 km/my) from ages  
355 of volcanic rocks. The predicted migration rates in our models are slightly  
356 higher than those predicted by conductive models alone (Roy et al., 2009),  
357 as they are enhanced by advective heating due to asthenosphere flow.

358 In contrast, at the downwind sector (the NE quadrant) the distinct lack of  
359 magmatic encroachment (Roy et al., 2009) is consistent with higher dynamic  
360 pressures and therefore melt exclusion from this part of the plateau (Figure  
361 5). Alternatively, the lack of magmatic encroachment on the NE margin  
362 of the Colorado Plateau may be due to the lower-magnitude of extension  
363 in the northern Rio Grande rift (Chapin and Cather, 1994) which results  
364 in smaller contrast in lithosphere thickness across the plateau margin. Our  
365 models predict a long-lived pattern of melt-exclusion from the downwind



366 sector of the plateau and protracted magmatism immediately outside the  
367 margin of the plateau (Figures 4 & 5). These predictions are consistent with  
368 the voluminous and long-lived magmatic centers of the middle-Tertiary to  
369 Neogene San Juan Volcanic Field (Lipman and Glazner, 1991) located NE of  
370 the plateau, outside its physiographic boundary. The northern margin of the  
371 plateau (adjacent to the Archean Wyoming Province) lacks magmatism and  
372 the relatively high upper mantle seismic wave speeds of the plateau interior  
373 continue into the Wyoming Province to the north. The transition into the  
374 Wyoming Province is therefore consistent with a more uniform lithosphere  
375 thickness.

### 376 *3.1.2. Properties of the Colorado Plateau lithosphere.*

377 Central to the idea of middle-Tertiary to Present melt-infiltration and  
378 magma migration into the margins of the Colorado Plateau is the excess  
379 thickness of the lithosphere beneath the Colorado Plateau relative to its sur-  
380 roundings. In the models explored here, asthenospheric flow around protrud-  
381 ing regions of thicker lithosphere sets up the key dynamic pressure gradients  
382 that are responsible for organizing melt-migration. Evidence for thicker litho-  
383 sphere beneath the Colorado Plateau relative to its surroundings is provided  
384 by a range of seismic observations (Schmandt and Humphreys, 2010; Lin and  
385 Ritzwoller, 2011; Sine et al., 2008; West et al., 2004; Levander and Miller,  
386 2012) and by xenolith data (Smith, 2000; Lee et al., 2001).

387 The magmatic infiltration process described here is further supported  
388 by the distinct geologic and geophysical contrast between the margins and  
389 the interior of the Colorado Plateau. The asthenosphere beneath the Rio  
390 Grande rift and the Basin and Range exhibit extremely low shear velocities

391 (e.g., West et al., 2004; Yang et al., 2008; Rau and Forsyth, 2011), suggestive  
392 of ubiquitous partial melt surrounding the plateau. Detailed seismic imaging  
393 clearly demonstrates that these low relative velocities extend significantly un-  
394 der the margins of the plateau, well inside the outer plateau’s physiographic  
395 boundary (Schmandt and Humphreys, 2010; Sine et al., 2008). In contrast,  
396 the interior of the plateau is seismically faster, with lower  $V_p/V_s$  ratios, than  
397 its margins (Schmandt and Humphreys, 2010; Humphreys and Dueker, 1994;  
398 Goes and van der Lee, 2002; Gao et al., 2004; Sine et al., 2008; Li et al., 2007).  
399 The plateau margins are also characterized by higher average surface heat-  
400 flow (Eggleston and Reiter, 1984; Swanberg and Morgan, 1985) and enhanced  
401 electrical conductivity in the upper mantle (Wannamaker et al., 2008). The  
402 spatial correlation between the regions of magmatism at the plateau margins  
403 and the observed geophysical structure (Figure 1), strongly suggests that the  
404 margins of the plateau have been modified by melt-infiltration and migration  
405 via processes akin to those explored in our models.

406 Within the higher-velocity plateau interior, recent studies image a local-  
407 ized region of fast seismic velocities to a depth of over 200 km adjacent to  
408 the Utah Transition Zone (Schmandt and Humphreys, 2010; Sine et al., 2008;  
409 Levander et al., 2011), interpreted as a region of lithospheric delamination  
410 or a “drip” at the base of the plate (Levander et al., 2011). There are uncer-  
411 tainties with this interpretation, in particular with respect to the apparent  
412 lithosphere-asthenosphere boundary imaged near 150 km depth continuously  
413 across the drip region (Levander and Miller, 2012). However, given that  
414 delamination is a plausible explanation for the deep feature, we note that  
415 the melt-infiltration process may promote lithospheric destabilization and

416 downwelling. In particular, the feedback mechanisms between melt segrega-  
417 tion, viscosity reduction, and deformation described in section 2.2 provides  
418 a natural and self-consistent source for the localized weakening that is re-  
419 quired to drive delamination in the absence of lithospheric thickening. In  
420 this scenario, melt infiltration, migration, and associated magmatism drive  
421 the delamination process, rather than vice-versa.

422 The contrast between the plateau interior and its margins is also evi-  
423 dent in the petrology of mantle xenoliths from the Colorado Plateau region.  
424 Xenolith populations show a predominance of pyroxenite lithologies at the  
425 plateau margins relative to the interior (Roy et al., 2005), with evidence for  
426 melt-related metasomatic alteration of lherzolite into pyroxenite via interac-  
427 tion with fluids of silicate and carbonatite composition (Porreca and Selver-  
428 stone, 2006). These observations raise the possibility that the seismically-  
429 and petrologically-distinct margins of the Colorado Plateau are modified by  
430 the infiltration of melts, through a combination of thermal effects (as explored  
431 in our models) and also chemical changes, leading to a thermo-chemical cor-  
432 rosion of the lithosphere.

### 433 *3.1.3. Relationship between magmatism and strain rate.*

434 The melt-related lithospheric rejuvenation process proposed here involves  
435 *in situ* modification of the margins of the region of thick lithosphere and, to  
436 the extent that it is controlled by the shape of the base of North America, it  
437 must also depend on the history of extension surrounding the plateau (Figure  
438 6a). Although in our models the lithosphere is not undergoing concurrent  
439 extension and warming, we note intriguing relationships between the pattern  
440 of magmatic encroachment and present-day strain-rates.

441 In particular, if melt-segregation and extraction is a strong function of  
442 the SDS feedback between matrix viscosity, permeability, and strain-rate (see  
443 2.2), then we would expect that melt-segregation into planar bands and melt-  
444 migration and extraction along melt bands will be most efficient in regions of  
445 highest strain rate (Figure 6b, c, &d). The present-day strain rate field across  
446 the Colorado Plateau is characterized by limited extension at the plateau  
447 margins, with the exception of the NW margin at the Utah Transition Zone  
448 between the plateau and the Great Basin (Kreemer et al., 2010; Berglund  
449 et al., 2012). Current strain-rates are highest at this margin and are spatially  
450 correlated with seismicity and magmatism. We would expect that SDS would  
451 most efficiently segregate melt along the NW margin, allowing channelized  
452 melt-transport. This focusing effectively *reduces* the percolative corrosion at  
453 greater depths predicted in the models, by enhancing the transport upwards  
454 along the LAB (Figure 6c), focusing and enhancing thermochemical corrosion  
455 at shallower depths because of the increased degree of thermal and chemical  
456 disequilibrium between the melt and the lithospheric mantle. This effect  
457 may explain the dramatic gradients in seismic velocity observed at the NW  
458 margin of the plateau (Schmandt and Humphreys, 2010), and the reduced  
459 magmatic encroachment in this quadrant compared to the SW (upwind)  
460 margin (4.0 km/my as opposed to 6.3 km/my (Roy et al., 2009)). Magneto-  
461 telluric measurements of the polarization anisotropy of electrical resistivity  
462 within the Utah Transition Zone are consistent with the presence of N-S  
463 oriented partial melt lenses, parallel to the plateau margin (Wannamaker  
464 et al., 2008), further supporting the role of SDS in this region.

465 The broad range of observations discussed above, including the patterns

466 of magmatism, heatflow, seismic and electrical structure, and xenolith data,  
467 suggest that the margins and likely the base of the thicker Colorado Plateau  
468 lithosphere has undergone variable thermo-chemical modification, driven by  
469 melt-infiltration. The distribution and rates of melt-infiltration are likely  
470 modulated by gradients in lithospheric thickness and strain-rates at the  
471 lithosphere-asthenosphere boundary. In the following we consider the im-  
472 plications of this process within the broader context of the western US and  
473 suggest that the thermo-chemical corrosion mechanism proposed here may  
474 be regionally significant.

475 *3.2. Application to the Cenozoic evolution of the western US and beyond.*

476 Following removal of the Farallon slab and the subsequent introduction  
477 of fresh asthenosphere material beneath the western US (Humphreys et al.,  
478 2003), we speculate that melt-related rejuvenation may have occurred on  
479 a regional scale at the margins and at the base of regions of thicker litho-  
480 sphere. Introduction of hot asthenosphere (e.g., “sub-EPR asthenosphere”  
481 in Figure 6a) triggers a spatially-variable melt-infiltration and rejuvenation  
482 of the North American plate. Specifically, the melt-infiltration and thermo-  
483 chemical modification inferred for the margins of the Colorado Plateau may  
484 have also affected the previously thick lithosphere of the now-extended Basin  
485 and Range Province and may have variably affected the thicker Wyoming  
486 craton to the north. Evidence that interaction with a LILE-rich melt or  
487 fluid resulted in re-enrichment of incompatible trace elements in the lower  
488 lithosphere and within the Great Falls Tectonic Zone at the margin of the  
489 Wyoming craton (Carlson et al., 2004) suggests that metasomatism may play  
490 a key role in the evolution of this region.

491 In this view, the continuous region of present-day higher seismic wavespeeds  
492 encompassing both the interior of the Colorado Plateau and Wyoming Province  
493 (e.g., Tian et al., 2009; Schmandt and Humphreys, 2010; Levander et al.,  
494 2011; West et al., 2004; Lin and Ritzwoller, 2011; Xue and Allen, 2010; Wag-  
495 ner et al., 2010; Sigoch, 2011), represents thicker portions of the lithosphere  
496 that has been only partially affected by melt-infiltration (Figure 6c). In  
497 contrast, the thinner, seismically slow lithosphere of the Basin and Range  
498 province may have been more completely rejuvenated and destabilized by  
499 melt-infiltration. The importance of partial melt within the seismically slow  
500 Basin and Range province is underscored by low shear wave speeds (Rau  
501 and Forsyth, 2011) and by higher  $V_p/V_s$  ratios (Schmandt and Humphreys,  
502 2010).

503 Thinking beyond the western US, we note that recent work in several  
504 localities, including the Ordos block of the North China craton (Menzies  
505 et al., 2007; Kusky et al., 2007), the eastern part of the Sino-Korean craton  
506 (O'Reilly et al., 2001), and the Tanzania craton (Wölbern et al., 2012) has  
507 suggested that within tectonically stable plate interiors, melt-infiltration and  
508 its effects can lead to rejuvenation and destabilization. These studies infer  
509 that melt-infiltration and its thermo-chemical consequences can transform  
510 previously stable, cratonic provinces into tectonized, orogenic zones. In the  
511 North China craton, for example, interaction of the lithosphere with infiltrat-  
512 ing melts is inferred to play a key role in the evolution of the eastern part of  
513 the craton from a region with a cool geotherm and a thick, highly magnesian  
514 keel into a tectonized zone characterized by present-day low upper-mantle  
515 seismic velocities and thin lithosphere (Menzies et al., 2007). In Tanzania, a

516 mid-lithosphere discontinuity imaged by S-wave receiver functions forms the  
517 upper boundary of a zone of reduced shear wave speeds in the lower litho-  
518 sphere (Wölbern et al., 2012). In this study, the lower lithosphere is inferred  
519 to have been modified by melt-infiltration and accompanying alteration of  
520 mineral assemblages (Wölbern et al., 2012), in a process akin to that inferred  
521 for the Wyoming Province (Carlson et al., 2004). We speculate, therefore,  
522 that melt-infiltration and thermo-chemical alteration may play an impor-  
523 tant role in the general evolution of continental interiors, particularly at the  
524 margins of thicker cratonic lithosphere.

#### 525 **4. Conclusions**

526 The well-studied Colorado Plateau region provides a unique laboratory for  
527 investigating processes by which stable continental interiors may be destabi-  
528 lized, namely, thermal and chemical modification during infiltration of melts  
529 or metasomatic fluids into the lithosphere. To first-order, the geometry of  
530 the lithosphere-asthenosphere boundary controls dynamic pressure gradients  
531 due to deformation, which in turn control the spatial distribution of melt-  
532 extraction and the observed distribution of magmatism. For a region of  
533 thicker lithosphere that protrudes into the “mantle wind”, such as the Col-  
534 orado Plateau, the dynamic pressures are lowest on the upwind side and  
535 highest on the downwind side. In this scenario, the highest rates of melt-  
536 infiltration and magmatic encroachment occur in the upwind sector of the  
537 plateau (its SW quadrant), whereas magmatic encroachment occurs at a  
538 slower rate on the NW and SE quadrants. In contrast, the downwind sec-  
539 tor (NE margin, adjacent to the San Juan volcanic field and northern Rio

540 Grande rift) shows a distinct lack of magmatic encroachment, consistent with  
541 our melt-extraction models. The melt-infiltration and rejuvenation process  
542 explored here provides a unifying framework for explaining both the observed  
543 asymmetry in magmatic patterns and also the observed geophysical contrasts  
544 between the plateau interior and its margins. Stress-driven melt segregation  
545 may play an important role in enhanced melt transport at the highest strain-  
546 rate NW margin of the plateau. In the Utah Transition Zone for example,  
547 sharp lateral seismic velocity and electrical conductivity gradients in the up-  
548 per mantle may be due to the presence of segregated melt in oriented planar  
549 bands.

550 We speculate that destabilization and rejuvenation of the lithosphere by  
551 melt-infiltration may have played a regionally important role in the Ceno-  
552 zoic evolution of the western US. For example, geochemical observations in  
553 the Wyoming Province suggest that the lower lithosphere in the region may  
554 have been partially modified by interaction with melts and metasomatic flu-  
555 ids. The seismically-fast interior of the Colorado Plateau and the adjacent  
556 Wyoming craton to the north may be portions of thicker North American  
557 lithosphere that have been less affected by melt-infiltration. In contrast, the  
558 margins of the Colorado Plateau and the thinned lithosphere of the Great  
559 Basin represent rejuvenated portions of the plate, both thermally and chemi-  
560 cally modified by interaction with melts. Feedback between melt segregation,  
561 viscosity reduction, and deformation provides a natural and self-consistent  
562 means of weakening the lithosphere in the western US and may have hastened  
563 its thinning by a combination of extension and convective removal. Melt-  
564 infiltration and accompanying rejuvenation may have played an important



565 role in the evolution of other continental interiors, such as the Sino-Korean,  
566 North China and Tanzania cratons, suggesting its general importance for the  
567 of continents.

## 568 **5. Acknowledgments**

569 We thank A. Ringler for early FEM models and B. Schmandt and E.  
570 Humphreys for providing a slice through their tomography model for Figure  
571 1. We also thank M. Spiegelman and T. Plank for fruitful conversations on  
572 magma and the Colorado Plateau.

## 573 **References**

574 Alibert, C., 1990. Peridotite xenoliths from the western grand canyon and  
575 the thumb: a probe into the subcontinental mantle of the colorado plateau.  
576 *Journal of Geophysical Research* 99, 21605–21620.

577 Berglund, H.T., Sheehan, A.F., Murray, M.H., Roy, M., Lowry, A.R., Nerem,  
578 R.S., Blume, F., 2012. Distributed deformation across the rio grande rift,  
579 great plains, and colorado plateau. *Geology* 40, 23–26.

580 Bodinier, J.L., Garrido, C.J., Chanefo, I., Brugier, O., Gervilla, F., 2008.  
581 Origin of pyroxenite-peridotite veined mantle by refertilization reactions:  
582 Evidence from the ronda peridotite (southern spain). *Journal of Petrology*  
583 49.

584 Butler, S.L., 2012. Numerical models of shear-induced melt band formation  
585 with anisotropic matrix viscosity. *Physics of The Earth and Planetary*  
586 *Interiors* 200-201, 28–36.

- 587 Carlson, R.W., Irving, A.J., Schulzec, D.J., Jr, B.C.H., 2004. Timing of  
588 precambrian melt depletion and phanerozoic refertilization events in the  
589 lithospheric mantle of the wyoming craton and adjacent central plains  
590 orogen. *Lithos* 77.
- 591 Chapin, C.E., Cather, S.M., 1994. Tectonic setting of the axial basins of the  
592 northern and central Rio Grande rift. volume 291 of *Special Paper of the*  
593 *Geological Society of America*. Geological Society of America.
- 594 Daines, M., Kohlstedt, D., 1994. The transition from porous to channel-  
595 ized flow due to melt/rock reaction during melt migration. *Geophysical*  
596 *Research Letters* 21, 145–148.
- 597 Eggleston, R., Reiter, M., 1984. Terrestrial heat flow estimates from  
598 petroleum bottom hole temperature data in the colorado plateau and the  
599 eastern basin and range province. *Geological Society of America Bulletin*  
600 95, 1027–1034.
- 601 Elkins-Tanton, L.T., 2005. Continental magmatism caused by lithospheric  
602 delamination. *Special Paper - Geological Society of America* 388, 449–461.
- 603 Fischer, K.M., Ford, H.A., Abt, D.L., Rychert, C.A., 2010. The lithosphere-  
604 asthenosphere boundary. *Annual Review of Earth and Planetary Science*  
605 38, 551–575.
- 606 Gao, W., Grand, S., Baldrige, W.S., Wilson, D., West, M., Ni, J., Aster,  
607 R., 2004. Upper mantle convection beneath the central Rio Grande rift  
608 imaged by P and S wave tomography. *Journal of Geophysical Research*  
609 109.

- 610 Goes, S., van der Lee, S., 2002. Thermal structure of the north american up-  
611 permost mantle inferred from seismic tomography. *Journal of Geophysical*  
612 *Research* 107.
- 613 Holtzman, B.K., Groebner, N.J., Zimmerman, M.E., Ginsberg, S.B., Kohlstedt,  
614 D.L., 2003. Stress-driven melt segregation in partially molten rocks.  
615 *Geochem. Geophys. Geosyst* 4, 26.
- 616 Holtzman, B.K., Kendall, J.M., 2010. Organized melt, seismic anisotropy,  
617 and plate boundary lubrication. *Geochem. Geophys. Geosyst.* 11, Q0AB06.
- 618 Holtzman, B.K., King, D.S., Kohlstedt, D.L., 2012. Effects of stress-driven  
619 melt segregation on the viscosity of rocks. *Earth and Planetary Science*  
620 *Letters* 359-360, 184–193.
- 621 Holtzman, B.K., Kohlstedt, D.L., 2007. Stress-driven melt segregation and  
622 strain partitioning in partially molten rocks: Effects of stress and strain.  
623 *Journal of Petrology* 48, 2379–2406.
- 624 Humphreys, E.D., Dueker, K., 1994. Western US upper mantle structure. *J.*  
625 *Geophys. Res* 99.
- 626 Humphreys, E.D., Hessler, E., Dueker, K., Farmer, G.L., Erslev, E., Atwater,  
627 T., 2003. How laramide-age hydration of north american lithosphere by the  
628 farallon slab controlled subsequent activity in the western united states.  
629 *International Geology Review* 45, 575–595.
- 630 Katz, R.F., Spiegelman, M., Holtzman, B., 2006. The dynamics of melt and  
631 shear localization in partially molten aggregates. *Nature* 442, 676–679.

632 Kelemen, P.B., Whitehead, J., Aharonov, E., Jordahl, K., 1995. Experi-  
633 ments on flow focusing in soluble porous media, with applications to melt  
634 extraction from the mantle. *Journal of Geophysical Research* 100, 475–496.

635 King, D.S.H., Hier-Majumder, S., Kohlstedt, D.L., 2011a. An experimental  
636 study of the effects of surface tension in homogenizing perturbations in  
637 melt fraction. *Earth Planet Sc Lett* , 1–13.

638 King, D.S.H., Holtzman, B.K., Kohlstedt, D.L., 2011b. An experimental  
639 investigation of the interactions between reaction-driven and stress-driven  
640 melt segregation. 1. application to mantle melt extraction. *Geochemistry,*  
641 *Geophysics, Geosystems* submitted, 1–38.

642 Kohlstedt, D.L., Holtzman, B.K., 2009. Shearing melt out of the earth:  
643 An experimentalist’s perspective on the influence of deformation on melt  
644 extraction. *Annual Reviews of Earth and Planetary Sciences* 37, 561–93.

645 Kreemer, C., Blewitt, G., Bennett, R., 2010. Present-day motion and defor-  
646 mation of the colorado plateau. *Geophysical Research Letters* 37.

647 Kusky, T.M., Windley, B.F., Zhai, M.G., 2007. Tectonic evolution of the  
648 North China Block: from orogen to craton to orogen. Geological Society,  
649 London, *Special Publications* 280.

650 Lee, C.T., Yin, Q., Rudnick, R.L., Jacobsen, S.B., 2001. Preservation of  
651 ancient and fertile lithospheric mantle beneath the southwestern united  
652 states. *Nature* 411, 69–73.

- 653 Lenardic, A., Moresi, L.N., Mühlhaus, H., 2003. Longevity and stability of cra-  
654 tonic lithosphere: Insights from numerical simulations of coupled mantle  
655 convection and continental tectonics .
- 656 Leroux, V., Tommasi, A., Vauchez, A., 2008. Feedback between melt percola-  
657 tion and deformation in an exhumed lithosphere–asthenosphere boundary.  
658 *Earth and Planetary Science Letters* 274, 401–413.
- 659 Levander, A., Miller, M.S., 2012. Evolutionary aspects of lithosphere discon-  
660 tinuity structure in the western u.s. *Geochemistry, Geophysics, Geosystems*  
661 13.
- 662 Levander, A., Schmandt, B., Miller, M.S., Liu, K., Karlstrom, K.E., Crow,  
663 R.S., Lee, C.T.A., Humphreys, E.D., 2011. Continuing colorado plateau  
664 uplift by delamination-style convective lithospheric downwelling. *Nature*  
665 472, 461.
- 666 Li, X., Yuan, X., Kind, R., 2007. The lithosphere-asthenosphere boundary  
667 beneath the western united states. *Geophysical Journal International* 170.
- 668 Lin, F.C., Ritzwoller, M.H., 2011. Helmholtz surface wave tomography for  
669 isotropic and azimuthally anisotropic structure. *Geophysical Journal In-*  
670 *ternational* 186, 1104–1120.
- 671 Lipman, P.W., Glazner, A.F., 1991. Introduction to middle tertiary  
672 cordilleran volcanism – magma sources and relations to regional tecton-  
673 ics. *J. Geophysical Research* 96, 193–13.
- 674 Liu, L., Gurnis, M., 2010. Dynamic subsidence and uplift of the colorado  
675 plateau. *Geology* 38, 663–666.

- 676 Marchesi, C., Griffin, W.L., Garrido, C.J., Bodinier, J.L., O'Reilly, S.Y.,  
677 Pearson, N.J., 2010. Persistence of mantle lithospheric re-os signature  
678 during asthenospherization of the subcontinental lithospheric mantle: in-  
679 sights from in situ isotopic analysis of sulfides persistence of mantle litho-  
680 spheric re-os signature during asthenospherization of the subcontinental  
681 lithospheric mantle: insights from in situ isotopic analysis of sulfides from  
682 the ronda peridotite (southern spain). *Contributions to Mineralogy and*  
683 *Petrology* 159, 315–330.
- 684 McKenzie, D., 1984. The generation and compaction of partially molten  
685 rock. *Journal of Petrology* 25, 713–765.
- 686 Menzies, M., Xu, Y., Zhang, H., Fan, W., 2007. Integration of geologygeo-  
687 physics and geochemistry: A key to understanding the north china craton.  
688 *Lithos* 96, 1–21.
- 689 Molnar, P., Jones, C., 2004. A test of laboratory based rheological param-  
690 eters of olivine from an analysis of late Cenozoic convective removal of  
691 mantle lithosphere beneath the Sierra Nevada, California, USA. *Geophys-*  
692 *ical Journal International* 156, 555–564.
- 693 Moucha, R., Forte, A.M., Rowley, D.B., Mitrovica, J.X., Simmons, N.A.,  
694 Grand, S.P., 2008. Mantle convection and the recent evolution of the  
695 colorado plateau and the rio grande rift valley. *Geology* 36, 439–442.
- 696 O'Reilly, S.Y., Griffin, W.L., Djomani, Y.H.M., Paul, 2001. Are litho-  
697 spheres forever? Tracking changes in the subcontinental lithospheric man-  
698 tle through time. *GSA Today* 11, 4–10.

- 699 Porreca, C., Selverstone, J., 2006. Pyroxenite xenoliths from the rio puerco  
700 volcanic field, new mexico: Melt metasomatism at the margin of the rio  
701 grande rift. *Geosphere* 2, 333–351;.
- 702 Rau, C.J., Forsyth, D.W., 2011. Melt in the mantle beneath the amagmatic  
703 zone, southern nevada. *Geology* 39, 975–978.
- 704 Roy, M., Jordan, T.H., Pederson, J., 2009. Cenozoic magmatism and rock up-  
705 lift of the colorado plateau by warming of chemically buoyant lithosphere.  
706 *Nature* 459.
- 707 Roy, M., MacCarthy, J.K., Selverstone, J., 2005. Upper mantle structure be-  
708 neath the eastern colorado plateau and rio grande rift revealed by bouguer  
709 gravity, seismic velocities, and xenolith data. *Geochemistry Geophysics*  
710 *Geosystems* 6.
- 711 Schmandt, B., Humphreys, E.D., 2010. Complex subduction and small-  
712 scale convection revealed by body-wave tomography of the western United  
713 States upper mantle. *Earth and Planetary Science Letters* 297.
- 714 Schmeling, H., Wallner, H., 2012. Magmatic lithospheric heating and weaken-  
715 ing during continental rifting: A simple scaling law, a 2-d thermomechanical  
716 rifting model and the east african rift system. *Geochemistry Geophysics*  
717 *Geosystems* 13.
- 718 Sigoch, K., 2011. Mantle provinces under north america from multifrequency  
719 p wave tomography. *Geochemistry, Geophysics, Geosystems* 12.
- 720 Silver, P.G., Holt, W.E., 2002. The mantle flow field beneath western north  
721 america. *Science* 295, 1054–1057.

- 722 Sine, C.R., Wilson, D., Gao, W., Grand, S.P., Aster, R., Ni, J., Baldrige,  
723 W.S., 2008. Mantle structure beneath the western edge of the Colorado  
724 Plateau. *Geophysical Research Letters* 35.
- 725 Smith, D., 2000. Insights into the evolution of the uppermost continental  
726 mantle from xenolith localities on and near the Colorado Plateau and re-  
727 gional comparisons. *Journal of Geophysical Research* 105, 16769–16781.
- 728 Soustelle, V., A.Tommasi, Bodinier, J.L., Garrido, C.J., A.Vauchez, 2009.  
729 Deformation and reactive melttransport in the mantle lithosphere above a  
730 large-scale partial melting domain: the ronda peridotite massif, southern  
731 spain. *Journal of Petrology* 50, 1235–1266.
- 732 Spiegelman, M., 1993. Flow in deformable porous media. part 1 simple  
733 analysis. *Journal of Fluid Mechanics* 247, 17–38.
- 734 Spiegelman, M., 2003. Linear analysis of melt band formation by simple  
735 shear. *Geochemistry Geophysics Geosystems* 4.
- 736 Swanberg, C.A., Morgan, P.M.P., 1985. Silica heat flow estimates and heat  
737 flow in the colorado plateau and adjacent areas. *Journal of Geodynamics*  
738 3, 65–85.
- 739 Takei, Y., Hier-Majumder, S., 2009. A generalized formulation of interfacial  
740 tension driven fluid migration with dissolution/precipitation. *Earth and*  
741 *Planetary Science Letters* 288, 138–148.
- 742 Takei, Y., Holtzman, B.K., 2009. Viscous constitutive relations of solid-  
743 liquid composites in terms of grain boundary contiguity: 3. causes and  
744 consequences of viscous anisotropy. *J. Geophys. Res.* 114, 23.



- 745 Tian, Y., Sigloch, K., Nolet, G., 2009. Multiple-frequency sh-wave tomog-  
746 raphy of the western us upper mantle. *Geophysical Journal International*  
747 178, 1384–1402.
- 748 Wagner, L., Forsyth, D.W., Fouch, M.J., James, D.E., 2010. Detailed three-  
749 dimensional shear wave velocity structure of the northwestern united states  
750 from rayleigh wave tomography. *Earth and Planetary Science Letters* 299.
- 751 Wang, Y., Forsyth, D., Rau, C., Carriero, N., Schmandt, B., Gaherty, J.,  
752 Savage, B., . Fossil slabs attached to unsubducted fragments of the farallon  
753 plate. Submitted for publication.
- 754 Wannamaker, P.E., Hasterok, D.P., Johnston, J.M., Stodt, J.A., Hall,  
755 D.B., Sodergren, T.L., Pellerin, L., Maris, V., Doerner, W.M., Unsworth,  
756 K.A.G.M.J., 2008. Lithospheric dismemberment and magmatic processes  
757 of the great basin–colorado plateau transition, utah, implied from magne-  
758 totellurics. *Geochemistry Geophysics Geosystems* 9.
- 759 Wenrich, K.J., et al., 1995. Spatial migration and compositional changes of  
760 Miocene-Quaternary magmatism in the western Grand Canyon. *Journal*  
761 *of Geophysical Research* 100, 10417–10440.
- 762 West, J.D., Fouch, M.J., Roth, J.B., Elkins-Tanton, L.T., 2009. Vertical  
763 mantle flow associated with a lithospheric drop beneath the Great Basin,  
764 *Nature Geoscience*. DOI:10 1038/.
- 765 West, M., Ni, J., Baldrige, W., Wilson, D., Aster, R., Gao, W., Grand,  
766 S., 2004. Crust and upper mantle shear-wave structure of the southwest

767 United States: Implications for rifting and support for high elevation. *J.*  
768 *Geophys. Res.* 109.

769 van Wijk, J., Baldrige, W., van Hunen, J., Goes, S., Aster, R., Coblenz,  
770 D., Grand, S., Ni, J., 2010. Small-scale convection at the edge of the  
771 colorado plateau: Implications for topography, magmatism, and evolution  
772 of proterozoic lithosphere. *Geology* 38, 611–614.

773 Wölbern, I., Rümpker, G., Link, K., Sodoudi, F., 2012. Melt infiltration  
774 of the lower lithosphere beneath the tanzania craton and the albertine  
775 rift inferred from s receiver functions. *GEOCHEMISTRY GEOPHYSICS*  
776 *GEOSYSTEMS*, in press .

777 Xue, M., Allen, R.M., 2010. Mantle structure beneath the western united  
778 states and its implications for convection processes. *Journal of Geophysical*  
779 *Research* B07303.

780 Yang, Y., Ritzwoller, M.H., Lin, F.C., Moschetti, M.P., Shapiro, N.M., 2008.  
781 Structure of the crust and uppermost mantle beneath the western united  
782 states revealed by ambient noise and earthquake tomography. *Journal of*  
783 *Geophysical Research* 113.

784 Zandt, G., Carrigan, C., 1993. Small-scale convective instability and upper  
785 mantle viscosity under california small-scale convective instability and up-  
786 per mantle viscosity under california small-scale convective instability and  
787 upper mantle viscosity under california small-scale convective instability  
788 and upper mantle viscosity under california. *Science* 261, 460–463.

789 Zhong, S., Zuber, M.T., Moresi, L., Gumis, M., 2000. Role of temperature-  
790 dependent viscosity and surface plates in spherical shell models of mantle  
791 convection. *Journal of Geophysical Research* 105, 11,063–11,082.

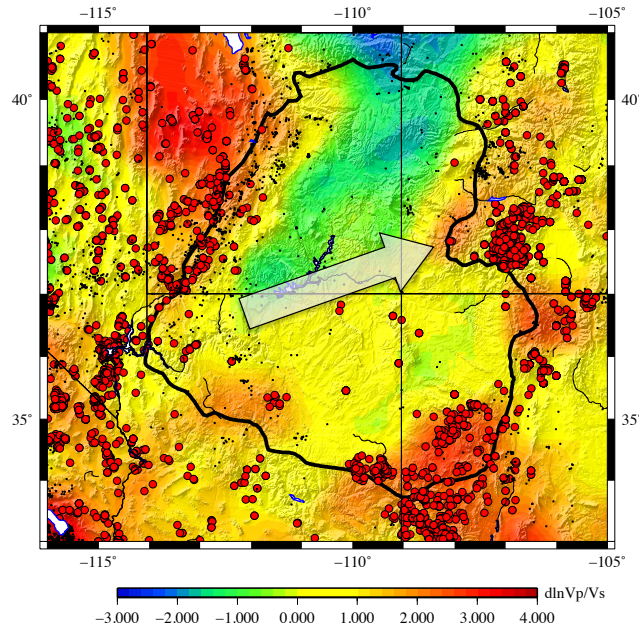


Figure 1: A composite image of the Colorado Plateau region (thick black line marks the physiographic boundary of the plateau) with published  $V_p/V_s$  ratios (color image) at 90 km depth, modified from Schmandt and Humphreys (2010). Large red circles indicate Cenozoic volcanic rocks in the NAVDAT database and small black dots indicate seismicity. Greater seismicity and magmatism at the margins of the plateau coincides with regions of higher  $V_p/V_s$  ratio relative to the interior. Large arrow indicates the direction of motion of the underlying asthenosphere in a reference frame stationary with respect to North America inferred from a combination of kinematic data and seismic anisotropy (Silver and Holt, 2002).

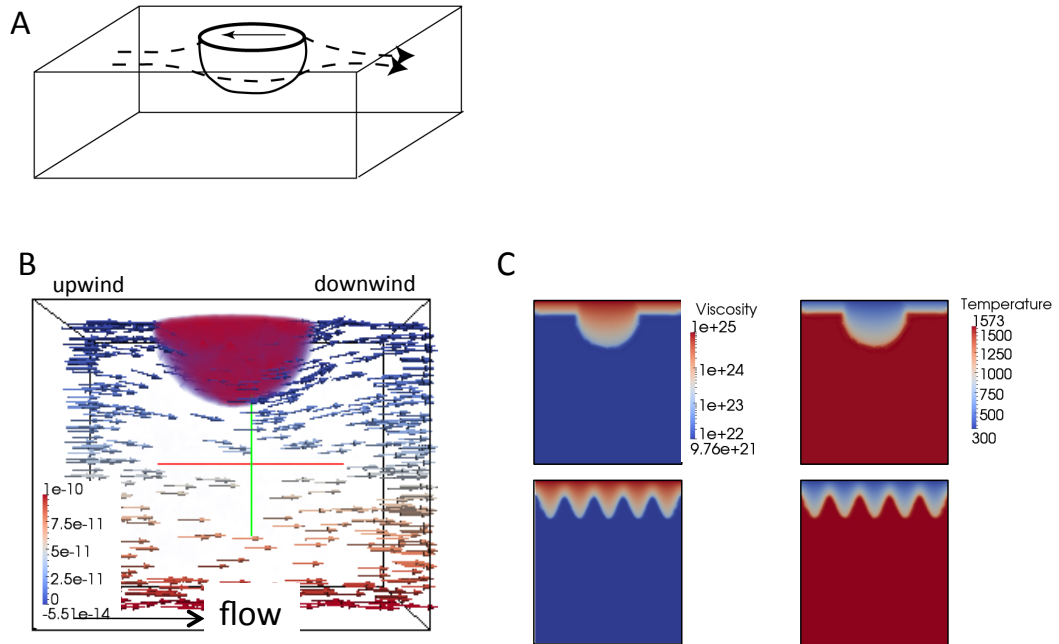


Figure 2: A. Cartoon of model showing a hemispherical region of thick, high-viscosity lithosphere protruding into lower-viscosity asthenosphere that flows from left to right. B. Kinematic boundary conditions at the base of the model drive flow in the asthenosphere around the high-viscosity protrusion, represented as a red hemispherical volume. The model domain is 1200 km by 1200 km by 1000 km (depth), with the hemisphere radius=300 km in this calculation. The bottom boundary is driven from left to right at  $\sim 10^{-9}$  m/s (red arrows) while the top boundary is held fixed. The steady-state flow field is shown for a slice through the center of the model, with velocity vectors color-coded by magnitude in m/s. C. Initial viscosity (Pa s) and temperature (K) structures in 2D models for a semicircular lithospheric protrusion (top) and for periodic ridges at the base of the plate (bottom).

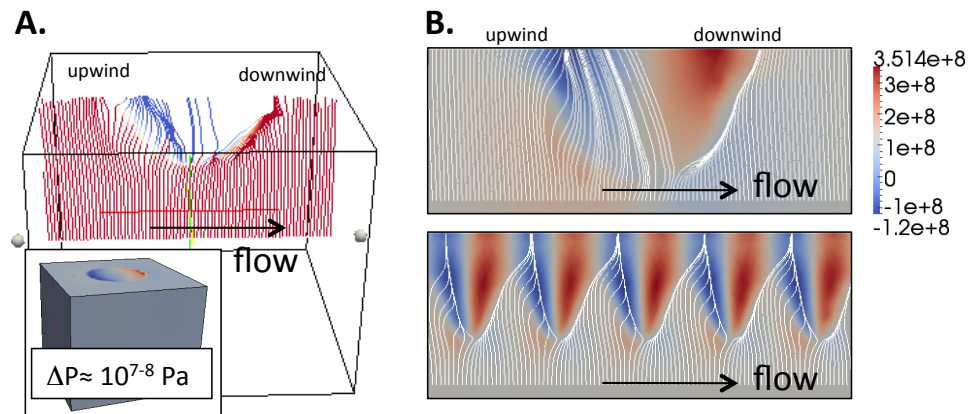


Figure 3: A. Melt extraction streamlines calculated from the flow field in Figure 2B, colored red when the line is outside the hemispherical keel and blue when it is within the keel. The pattern of melt-extraction illustrates primarily upward flow, dominated by buoyancy of the melt, but with significant lateral diversions due to dynamic pressure gradients (illustrated in the inset) that drive melt into the keel on the “upwind” side and suck melt away from the keel on its “downwind” side. B. Melt extraction streamlines calculated for the semicircle and periodic ridges in Figure 2C, showing the persistent asymmetry in dynamic pressures (in Pa) with calculated melt streamlines superimposed in white.

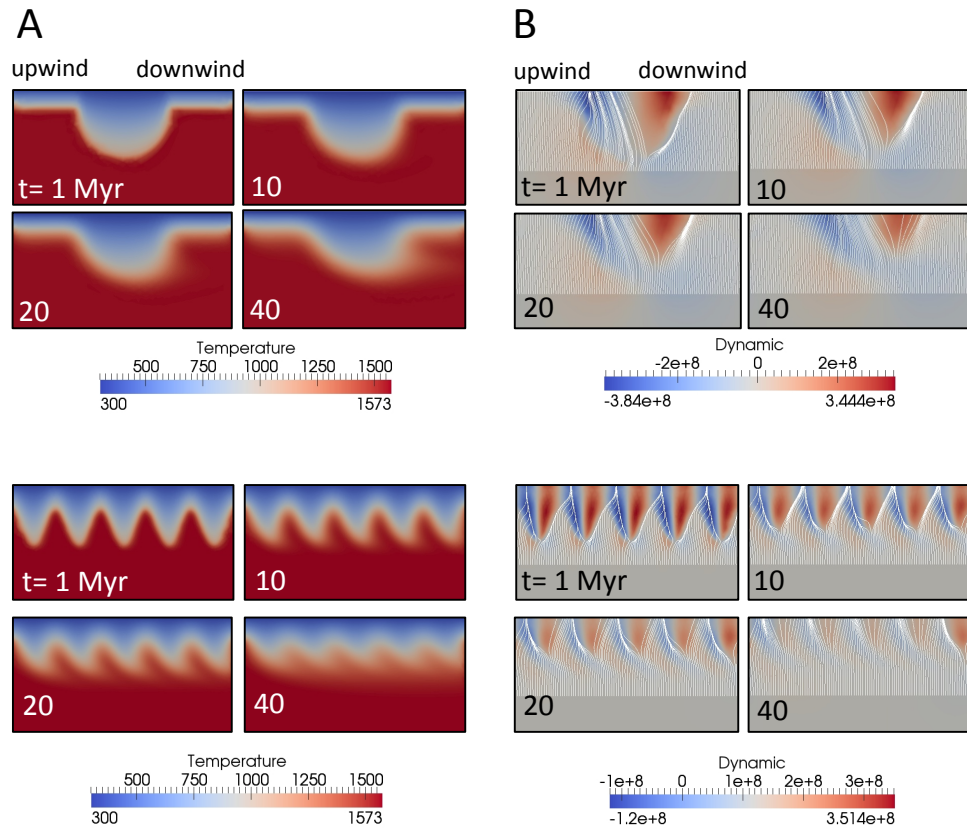


Figure 4: A. Temporal evolution of the temperature (A, in K) and dynamic pressure (B, in Pa) fields and accompanying changes in melt extraction through time. Results are shown for semicircular protrusions (top panels) and periodic ridges (bottom panels). The effects of temperature dependent viscosity and a combination of advective and conductive heating may be seen for tens of millions of years, leading to a persistent upwind-downwind asymmetry in both dynamic pressures and in melt extraction.

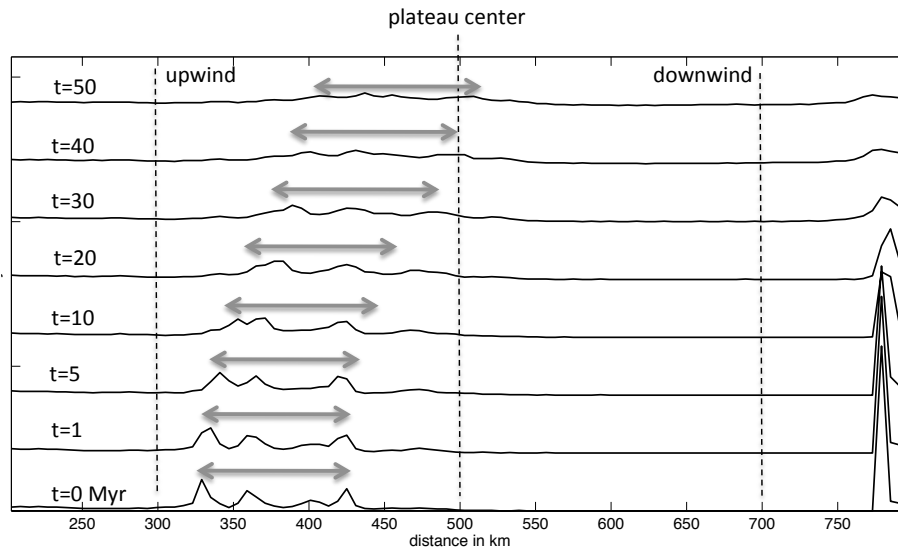


Figure 5: Plot of normalized streamline density at the surface (a measure of melt-focusing defined as the number of streamlines per km at the surface, normalized by the value at depth below the keel) as a function of time for the semicircular protrusion model shown in Figure 4B. The vertical dashed lines indicate the edges (at 300 and 700 km) and the center (at 500 km) of the semi-circular protrusion. This calculation shows the inward migration of the zone of melt-focusing on the upwind side of the protrusion (indicated by grey double arrows) toward the center of the protrusion. On the downwind side, there is a persistent exclusion of melt streamlines (and lack of migration).



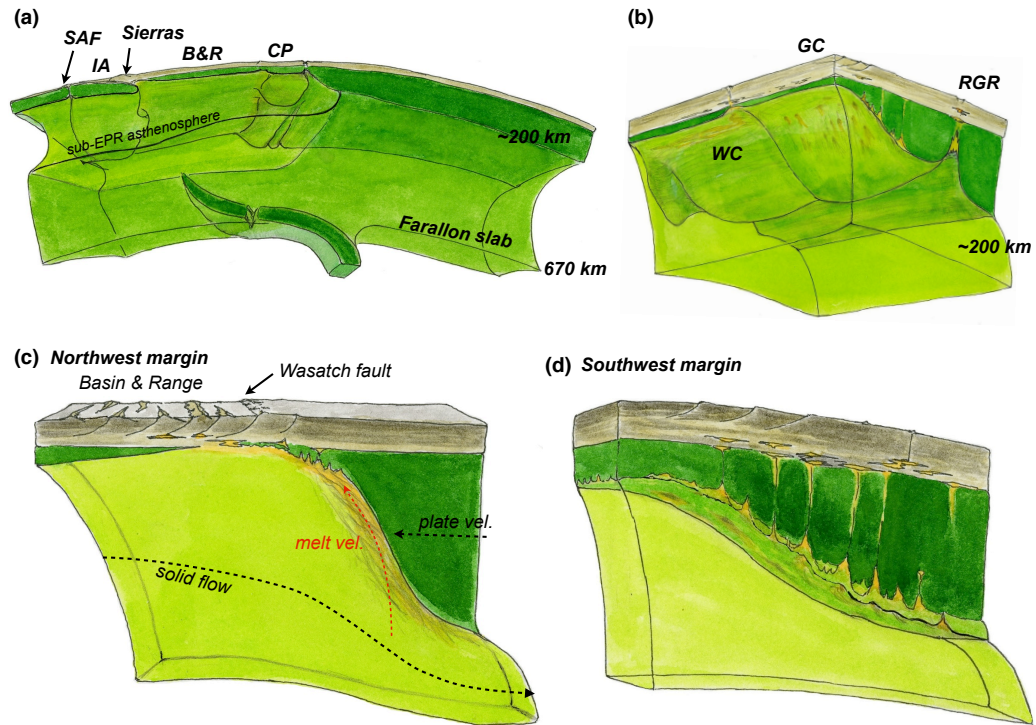


Figure 6: (a) Cartoon illustrating the geodynamic context for the Colorado Plateau within the western US. Cenozoic evolution of the western US is characterized by removal and fragmentation of the Farallon slab, followed by possible replacement of the sub-lithospheric mantle by warm, sub-EPR asthenosphere (e.g., Moucha et al., 2008); WC=Wyoming craton; CP=Colorado Plateau; SAF=San Andreas Fault; B&R=Basin and Range; IA=Isabella Anomaly, a possible remnant of the Farallon slab (Wang et al.). (b) The keel of the Colorado Plateau viewed from below, looking roughly NE (GC=The Grand Canyon; RGR=Rio Grande Rift). The keel may have significantly different character on the LAB at the NW margin as compared to other margins, as shown in (c) and (d). (c) We hypothesize the presence of stress-driven melt segregation (SDS) along a steep LAB at the high strain-rate NW margin, characterized by sharp lateral contrasts in seismic wave speed and electrical conductivity. (d) At lower strain-rate margins, such as the SW margin, we hypothesize more diffuse zones of modification/corrosion; the absence of large degrees of SDS corresponds to the behavior modeled in this paper, with melt migrating dominantly upward but modified by dynamic pressure gradients in the keel.

Symbol	Variable	Values used
$\phi$	porosity	< 1% (low porosity limit)
$\kappa$	solid permeability	$10^{-15}$ to $10^{-12}$ m <sup>2</sup>
$\rho_f$	melt density	2800 kg/m <sup>3</sup>
$\rho_s$	solid density	3300 kg/m <sup>3</sup>
$\mathbf{u}$	melt velocity	calculated in Eqn. 1
$\mathbf{v}$	solid velocity	0 to 1.6 <sup>9</sup> m/s
$\eta, \eta_l, \eta_a$	solid shear viscosity	$10^{18}$ to $10^{25}$ Pa s
$\zeta$	solid bulk viscosity	0; no compaction in melt-streamline calculations
$\mu$	melt viscosity	1 Pa s
$P$	fluid pressure	hydrostatic pressures up to $4 \times 10^{10}$ Pa
$\mathbf{g}$	acceleration due to gravity	9.82 m/s <sup>2</sup>
$\eta_0$	reference viscosity	$10^{22}$ Pa s
$E$	activation parameter $E/R(\Delta T)^2$	$5.4 \times 10^{-3}$ /K

Table 1: Physical parameters in models